

# Exploring backup requirements to complement wind, solar and hydro generation in a highly renewable Spanish power system

P. Tapetado<sup>a,\*</sup>, M. Victoria<sup>b,c,\*\*</sup>, M. Greiner<sup>b,c</sup>, J. Usaola<sup>a</sup>

<sup>a</sup> Department of Electrical Engineering, Universidad Carlos III de Madrid, Leganés, Madrid, Spain

<sup>b</sup> Department of Engineering, Aarhus University, 8000, Aarhus C, Denmark

<sup>c</sup> ICLIMATE Interdisciplinary Centre for Climate Change, Aarhus University, Denmark

## ARTICLE INFO

### Keywords:

Renewable integration  
Backup generation  
Flexibility  
Interannual variability

## ABSTRACT

A weather-driven model is used to investigate the requirements for the backup generation (annual energy, power capacity and flexibility) in a power system with different penetrations of wind, solar photovoltaics, and hydroelectricity. The impact of interannual variability is assessed by using 26 years of weather data. The flexibility needed for the backup generation is found to be higher as the solar penetration increases since ramps caused by sunrises and sunsets are more significant than those caused by hour-to-hour wind fluctuations. The model is applied to the Spanish power system and two dispatch strategies for reservoir hydro and pumped hydro storage are evaluated. The currently installed gas power capacity is found to be sufficient to secure hourly demand for high renewable penetration.

## 1. Introduction

Power systems around the globe are rapidly changing pushed by the urgency to mitigate climate change but also pulled by the dramatic cost reduction experienced by renewable technologies. The Paris Agreement led the European Commission to propose a plan to achieve a climate-neutral economy by 2050 [1]. For 2030, European countries have developed their National Energy and Climate Plans (NECP), see e.g. Ref. [2], in which vast installation of wind and solar photovoltaic (PV) capacities are expected in the next decade.

Increasing the share of Variable Renewable Energy Sources (VRES), i.e., wind and solar PV, challenges the design and operation of power systems. The literature on highly renewable power systems includes weather-driven models based on heuristics rules [3–7] and techno-economic optimization where power capacities and hourly dispatches are jointly optimized [8–13]. The former include a limited number of generation and storage technologies and have proven to be extremely valuable to unveil the main system dynamics in a variety of scenarios: different renewable penetration, wind-solar mix, etc. The weather-driven model approach has been used to estimate backup energy and power capacities [5,6], storage [5], and transmission capacity requirements [7]. Our paper contributes to the existing literature on

weather-driven models by including: (1) hydroelectricity in the models, (2) two alternative dispatch strategies for hydro (storage-first and peak-shaving), (3) a simplified methodology to evaluate flexibility requirements for the backup generation time series. Moreover, the use of 26-year long weather time series, enables us to quantify the impact of interannual variability. We focus on the following research questions:

- What is the optimal wind-solar mix to minimize the required backup energy and capacity when hydroelectricity and storage are included?
- What is the flexibility required for backup energy in different scenarios?

Flexibility is defined as the backup generation ability to respond to the changes in hourly mismatch between VRES generation and demand [11]. Following [14], we use an “offline” index to assess the required flexibility. Then, we investigate the optimal composition of the fleet of backup power plants needed to provide the required flexibility.

\* Corresponding author.

\*\* Corresponding author. Department of Engineering, Aarhus University, 8000, Aarhus C, Denmark.

E-mail address: [ptapetad@ing.uc3m.es](mailto:ptapetad@ing.uc3m.es) (P. Tapetado).

<https://doi.org/10.1016/j.esr.2021.100729>

Received 20 December 2019; Received in revised form 4 September 2021; Accepted 7 October 2021

Available online 2 November 2021

2211-467X/© 2021 The Authors.

Published by Elsevier Ltd.

This is an open access article under the CC BY-NC-ND license

(<http://creativecommons.org/licenses/by-nc-nd/4.0/>).

## 2. Methodology

### 2.1. Renewable generation time series and mismatch

In the weather-driven methodology, the mismatch  $\Delta_{VRES}(t)$  is defined as

$$\Delta_{VRES}(t) = W(t) + S(t) - L(t) \quad (1)$$

where  $W(t)$  and  $S(t)$  are the wind and solar PV generation time series, and  $L(t)$  represents the electricity load. The wind fraction  $\alpha = \langle W \rangle / (\langle S \rangle + \langle W \rangle)$  represents the ratio between average wind and average VRES generation. The ratio between average VRES energy and average load defines the VRES penetration  $\gamma = (\langle S \rangle + \langle W \rangle) / \langle L \rangle$ .  $\langle \cdot \rangle$  denotes the average of the time series.

The time series for renewable technologies comprise 26-years (1991–2016) with hourly resolution. Wind and solar PV time series were obtained using reanalysis weather data, converted to electricity generation, and aggregated on country scale are openly available in Refs. [15,16]. For hydro, historical monthly values of inflow retrieved from Ref. [17] are used to estimate a constant hourly inflow per month. Load time series corresponding to years 2006–2016 are retrieved from Ref. [18]. They are duplicated to obtain load time series for the modeled period (1991–2016).

### 2.2. Modelling hydro and storage dispatch

When reservoir hydro and storage are included in the system, the mismatch  $\Delta(t)$  is defined as:

$$\Delta(t) = \Delta_{VRES}(t) + H(t) \quad (2)$$

where  $H(t)$  represents the dispatch of reservoir hydro and storage technologies. For reservoir hydro,  $H(t)$  is positive or zero. When representing a storage technology,  $H(t)$  is positive when the storage discharges and negative when it charges. The dispatch of reservoir hydro and storage can follow any of the two simplified strategies:

**Storage-first:** Whenever the VRES mismatch is positive, the excess generation is stored. In case of a negative VRES mismatch, the generation deficit is covered with stored energy. This strategy is proven to be optimal to minimize the required backup energy [4].

**Peak-shaving/Valley-filling:** For a negative mismatch interval, the energy released from the storage is distributed among the interval hours to reduce extreme mismatch values. This strategy assumes a perfect foresight to so that the length of the negative interval is known.

For reservoir hydro, the maximum cumulative hydro generation every month is limited by the monthly inflow. A detailed mathematical and graphical definition of storage strategies is provided in the Supplementary Materials. The time series  $H(t)$  are obtained by applying one of the two strategies to the technologies included in the scenario under analysis. For reservoir hydro, water inflow is used for charging, while for Pump Hydro Storage (PHS) and batteries, positive VRES mismatch is used for charging. When more than one storage technology is available, those with higher efficiency are dispatched first, *i.e.*, the dispatch order is batteries, PHS, reservoir hydro.

### 2.3. Backup energy, capacity and flexibility

Backup generation is needed to supply the residual load when wind, solar, storage, and reservoir hydro dispatches are not enough. The residual load  $\Delta_-(t) = -\min(\Delta(t), 0)$  is defined as the negative part of the mismatch time series in (2). The residual load can be provided by conventional units as Combined Cycle Gas Turbines (CCGT), Open Cycle Gas Turbines (OCGT), nuclear or coal power plants. The annual backup energy  $E_B$  is defined as the sum of residual loads, and the backup capacity  $C_B$  as the maximum value.

$$E_B = \sum_t \Delta_-(t) C_B = \max(\Delta_-(t)) \quad (3)$$

Following [14], the flexibility index  $f$  of the residual load is calculated by

$$f = \frac{1/2 \left[ \bar{P} - \underline{P} \right] + 1/4 \left[ \left( \bar{R} + \underline{R} \right) \cdot \delta t \right]}{\bar{P}} \quad (4)$$

where  $\bar{P}/\underline{P}$  is  $C_B$  or 0, respectively.  $\bar{R}/\underline{R}$  is the absolute maximum power increment/decrement in an hour ( $\delta t = 1$ ), also known as residual load ramp. A flexibility index of 1 denotes high residual load power variation between successive hours while  $f$  close to 0 indicates a smooth variation.

The optimal composition of the backup generation fleet is assessed through an optimization problem that consists in the minimization of the annualized capital and operational costs of the complete backup fleet. This objective is under two constraints: 1) The backup generation must supply the residual load at every hour. 2) The flexibility of the backup generation fleet  $FLEX^{BG}$  must be higher or equal to the flexibility  $f$  demanded by the residual load. The flexibility of the group of backup generation units is defined as:

$$FLEX^{BG} = \sum_{n \in BG} \left[ \frac{\bar{P}_n}{\sum_{n \in BG} \bar{P}_n} \cdot f_n \right] \quad (5)$$

where,  $P_n$  and  $f_n$  are the power capacity and flexibility of every unit  $n$ .  $f_n$  is estimated by applying equation (4) setting  $\bar{P}/\underline{P}$  as maximum/minimum power capacity of a unit  $n$  and  $\bar{R}/\underline{R}$  as ramping up/down capacity of a unit  $n$ .

### 2.4. Scenarios under analysis

Four different scenarios, which incorporate the technologies shown in Table 1, are investigated:

- Scenario 0. (Wind and solar). This scenario is a base case in which wind and solar PV are the only renewable technologies available, that is  $H(t) = 0$ .
- Scenario 1. (Wind, solar and hydro). Besides wind and solar PV, reservoir hydroelectricity is included as dispatchable technology.
- Scenario 2. (Wind, solar, PHS and hydro). This scenario adds PHS that can store energy from the grid. Scenario 2 includes the PHS capacity currently available at the Spanish power system.
- Scenario 3. (Wind, solar, batteries, PHS, and hydro). Batteries are added to Scenario 2.

## 3. Results and discussion

For Scenario 0, Fig. 1 shows the annual backup energy  $E_B$  as a function of VRES penetration  $\gamma$  and wind fraction  $\alpha$ . The red line depicts the optimal  $\alpha$  that minimizes the backup energy for every  $\gamma$ . The horizontal axis in Fig. 1 can be read as a pseudo-time evolution as it represents increasing VRES penetration in the power system. Minimum backup energy is achieved for high wind fractions since, in the absence of storage, increasing solar contribution will require significant backup

**Table 1**  
Reservoir hydro and storage characteristics.

	Power Capacity [GW]	Energy Capacity [GWh]	Efficiency
Reservoir hydro	17	26,500	0.84
PHS	3.5	73	0.84-0.84 = 0.7
Batteries	70	730	0.9-0.9 = 0.81

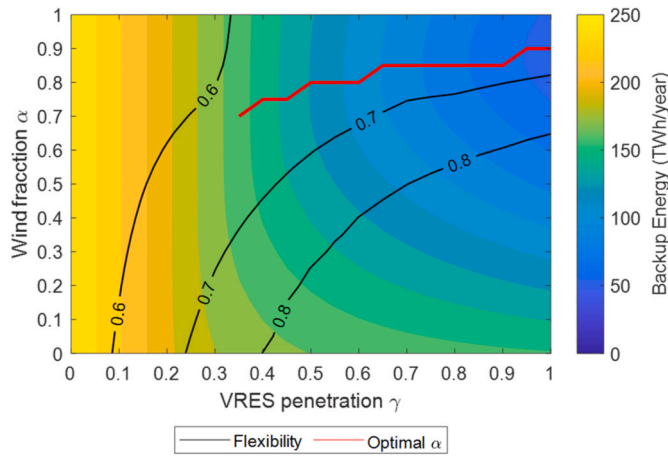


**Fig. 1.** Colourmap showing the annual backup energy  $E_B$  for Scenario 0 as a function of the VRES penetration  $\gamma$  and the wind fraction  $\alpha$  for the year 2016 in Spain. The red line represents the optimum  $\alpha$ , which minimizes  $E_B$  for every  $\gamma$ . Black lines represent the flexibility index  $f$  of the system as a function of  $\gamma$  and  $\alpha$ . Same figures for Scenarios 1, 2, and 3 are included in the Supplementary Materials.

generation during the nights.

Table 2 summarizes the results when the model is applied to the different scenarios and storage strategies. All the cases impose that the energy generated by VRES plus storage and hydro must be equal, on average, to the energy demand over the year. The latter implies that annual energy backup and curtailed energy are equal. For Scenario 0, this is equivalent to set  $\gamma = 1$ . For Scenario 1,  $\gamma$  is lower than 1 because hydro is not included in the definition of  $\gamma$ . Scenarios 2 and 3 require higher  $\gamma$  values than Scenario 1 because the round-trip efficiency of the storage technologies is lower than one, and this is compensated by a higher VRES generation. It should be remarked that, due to the presence of storage, Scenarios 2 and 3 are able to effectively supply a higher percentage of hourly demand with VRES energy, compared to Scenario 1. Regarding the wind to solar mix, Table 2 and Fig. 4 in Supplementary Materials show how the solar penetration increases (optimal  $\alpha$  is reduced) when dispatchable technologies are aggregated since they contribute to balancing the diurnal generation pattern of solar PV. Solar penetration is particularly benefited when short-cycle storage is used, as previously shown [4,19].

Regarding the results on the storage-first strategy, it is shown how annual backup energy decreases as dispatchable technologies are aggregated.  $E_B$  goes from 55 TWh in Scenario 0 to 6 TWh in Scenario 3. The percentage of the annual energy demand (252 TWh) covered with VRES, storage, and hydro, increases from 78.2% to 97.6%. To check that the operation of reservoir hydro is compatible with historical trends, Figs. 2 and 3 show the hydroelectricity generation and the filling level of hydro reservoirs. Scenarios 1 and 2 are very similar, because the energy

**Table 2**

Power system characteristics for different scenarios and storage dispatch strategies. The first two columns refer to backup generation to ensure hourly demand. Values upfront (in the parenthesis) correspond to storage-first (peak-saving) strategy. Average and standard deviation values for the 26 years considered are reported.

Strategy: Storage First (Peak Shaving)						
	Backup Power Capacity, $C_B$ [GW]	Annual Backup Energy, $E_B$ /Curtailed energy [TWh]	Demand covered with VRES + Hydro [%]	Flexibility, $f$	$\gamma$	$\alpha$
Scenario 0	33 ± 2 (33 ± 3)	55 ± 4 (55 ± 4)	78.2% (78.2%)	0.68 ± 0.03 (0.68 ± 0.03)	1.00 ± 0.00 (1.00 ± 0.00)	0.85 ± 0.05 (0.85 ± 0.05)
Scenario 1	33 ± 2 (20 ± 1)	42 ± 5 (42 ± 5)	83.3% (83.3%)	0.77 ± 0.04 (0.77 ± 0.05)	0.91 ± 0.03 (0.91 ± 0.03)	0.84 ± 0.05 (0.84 ± 0.05)
Scenario 2	33 ± 2 (19 ± 1)	36 ± 5 (36 ± 5)	85.7% (85.7%)	0.76 ± 0.04 (0.78 ± 0.06)	0.92 ± 0.03 (0.92 ± 0.03)	0.81 ± 0.05 (0.81 ± 0.05)
Scenario 3	27 ± 8 (12 ± 3)	6 ± 2 (4 ± 2)	97.6% (98.4%)	0.90 ± 0.04 (0.93 ± 0.08)	1.01 ± 0.02 (0.99 ± 0.03)	0.36 ± 0.07 (0.33 ± 0.07)

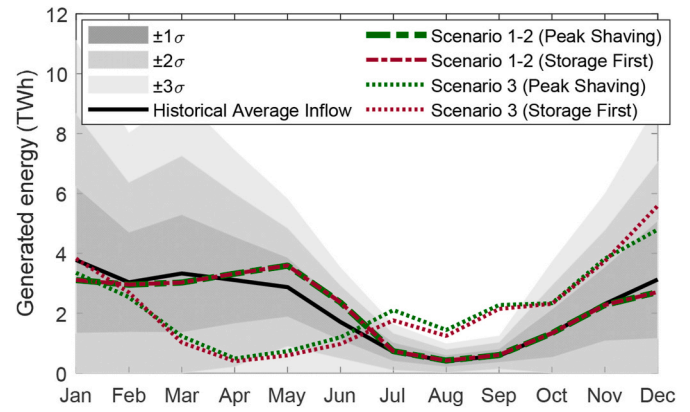


**Fig. 2.** Energy generated by reservoir hydro for Scenarios 1, 2 and 3 under the two different strategies. Black line represents the 26-years average monthly energy inflow for reservoir hydro power plants. Deviation in the historical data is indicated by the grey areas.

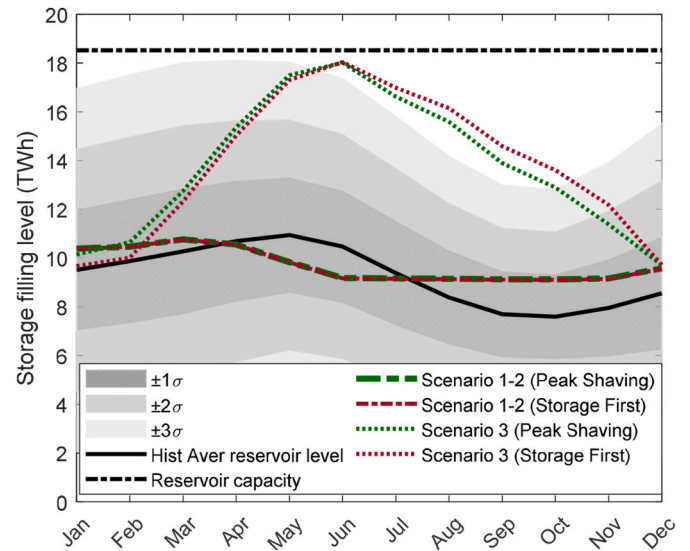


**Fig. 3.** Storage filling level for reservoir hydro for Scenarios 1, 2 and 3 under the two different storage strategies. Black line represents the average historical reservoir hydro filling level for the last 26 years. Grey areas represent the deviation of reservoir level for the 26 years considered.

capacity provided by PHS is small, and reservoir hydro resembles the historical operation. In Scenario 3, the presence of batteries operated also with storage-first strategy, together with a solar-dominant VRES generation, reduces the energy produced by reservoir hydro from February to June, which historically is a period with high

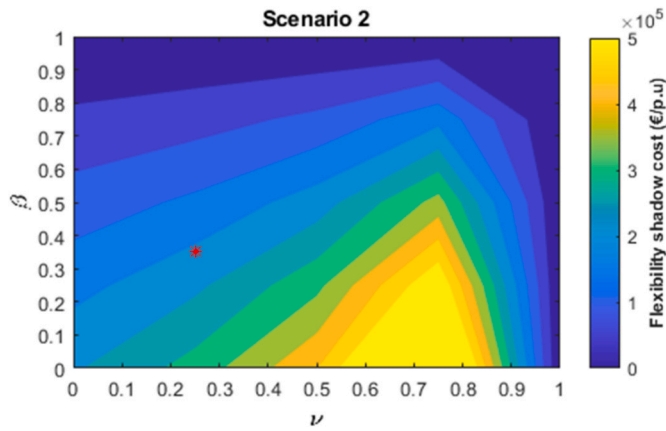


**Fig. 4.** Shadow cost associated with the flexibility constraint as a function of  $\beta$  and  $\nu$  in Scenario 2 with peak shaving strategy.  $\beta$  and  $\nu$  are the ratios between operational costs and flexibility, respectively, for the two kinds of power unit considered. The red star represents the  $\beta$  and  $\nu$  values for the case of example discussed in the text.

hydroelectricity production. Consequently, the filling level reaches higher values in those months, but it remains lower than the maximum energy capacity of reservoirs.

Using the peak-shaving strategy, the results for hydro dispatch is similar. Scenarios 1 and 2 are within the range of historical values for every month, while for Scenario 3, the filling level of hydro reservoirs is high in spring-summer months.

The described storage strategies represent two extreme behaviours for reservoir hydro. Storage-first strategy could be seen as naïve since it assumes that the hydro operator does not know the state of the system in successive hours, while peak-shaving strategy could be too optimistic since it assumes perfect foresight for the entire month. In principle, the Spanish reservoir hydro power plants operate somewhere between the two strategies.

The required backup power capacity shows the largest difference between strategies. If we focus on Scenario 2, the one resembling the technologies currently available in the Spanish power system,  $C_B$  is 33 GW for the storage-first strategy and 19 GW for the peak-shaving strategy. Since the current CCGT installed capacity in Spain is 26.4 GW [17], proper operation of existing reservoir hydro, PHS and CCGT power plants should be able to achieve significantly large VRES penetration in the system.

Fig. 1 also shows the flexibility index  $f$  of the residual load time series calculated with eq. (4).  $f$  increases with  $\gamma$  but decreases with  $\alpha$ , indicating that the diurnal generation pattern of solar PV has a higher impact on flexibility requirements than hourly fluctuations in wind generation. This is in agreement with [11].

Table 2 provides the flexibility index for the residual load in every scenario evaluated. As dispatchable technologies are incorporated into the system, the optimal solar penetration increases, and so does the flexibility index. Once the flexibility required by the residual demand in every scenario is estimated, the remaining question is what kind of power units are needed in the backup generation fleet to supply the residual load with the required flexibility. To answer this question, we apply the optimization problem, described in section 2.3 and mathematically in the Supplementary Materials. There are many types of power units with different cost and flexibility characteristics. For this reason, the optimization problem is defined as a function of the operational cost ratio  $\beta$ , and flexibility ratio  $\nu$  of two kinds of power units named as fast and slow units.

$$\beta = c^{\text{OPER slow unit}} / c^{\text{OPER fast unit}} \quad \nu = f^{\text{slow unit}} / f^{\text{fast unit}} \quad (6)$$

Fig. 4 shows the shadow cost, which is obtained by the dual Karush-Kuhn-Tucker variable of the flexibility constraint, for Scenario 2 under

the peak-shaving strategy. Equivalent figures for other scenarios and storage strategy are provided in the Supplementary Materials. The shadow cost represents the marginal cost of covering an incremental amount of flexibility, that is, it provides an indication of the impact of the flexibility constraint on the cost of the backup generation. For instance, when the fast power unit is assumed to be a CCGT power plant with  $f^{\text{fast unit}} = 0.8$  ( $\bar{P} = 100\%$ ,  $\underline{P} = 20\%$ ,  $\bar{R} = \underline{R} = 80\%/h$ ) and  $c^{\text{OPER fast unit}} = 57.5 \text{ €/MWh}$ , and the slow unit is assumed to be a nuclear power plant with  $f^{\text{slow unit}} = 0.2$  ( $\bar{P} = 100\%$ ,  $\underline{P} = 80\%$ ,  $\bar{R} = \underline{R} = 20\%/h$ ) with  $c^{\text{OPER slow unit}} = 20 \text{ €/MWh}$ ,  $\beta = 0.35$  and  $\nu = 0.25$  are obtained (red point on Fig. 4). This results into a shadow cost of flexibility of 0.23 ME.

However, it is interesting to realize that Fig. 4 depicts zero value for the shadow cost for some  $\beta$  and  $\nu$  combinations, which means that for such combinations, i.e. when slow and fast units are not very different, the flexibility constraint is not binding and it could be neglected when selecting the optimal backup fleet portfolio.

The simplified weather-driven modelling approach that we have used in this paper entails some limitations. The most significant are the reduced number of technologies and the fact that we do not consider cost optimization. The latter is the main driver in techno-economic optimization models. These limitations might result in a too idealized operation of the energy system. However, by keeping the model simple we can explore a wide range of possibilities in terms of wind and solar penetration and obtain general but also robust estimations of the need for energy and backup capacities.

#### 4. Conclusions

The weather-driven methodology has been applied to the Spanish power system. Our results indicate that a system with large renewable penetration is capable of supplying hourly electricity demand, confirming previous studies. Moreover, the parametrical sweeps implemented in this work provide new insights on the capacity and flexibility requirement of backup generation under different penetration of wind, solar and hydroelectricity. First, for high renewable penetrations, higher wind to solar ratio translates into lower backup energy required to secure the hourly supply. This remains true unless large capacities of high-efficiency short-term storage are available to compensate for the daily fluctuations in solar generation. In practice, this means that the deployment of electric batteries, either static or in electric vehicles, or the extension of Pumped Hydro Storage is necessary to allow high solar penetrations in the grid.

Second, as expected, the peak-shaving storage dispatch strategy reduces the required backup power capacity. This has a strong practical implication for the Spanish power system. Using that hydro dispatch strategy, the current CCGT power capacity would be enough to balance a system in which the sum of wind, solar, and hydro generation is, on average, equal to the electricity demand, even taking into consideration the interannual weather variability. Finally, we have found that the required flexibility for the backup generation increases with solar penetration because the predictable but significant power variation due to sunrises and sunsets induce higher ramps in the backup energy than those demanded by hour-to-hour wind fluctuations.

#### Declaration of competing interest

The authors declare that they have no known competing financial interests or personal relationships that could have appeared to influence the work reported in this paper.

#### Acknowledgements

Pablo Tapetado acknowledges the University Carlos III of Madrid (Ayudas para la Movilidad del Programa Propio de Investigación). M. Victoria, and M. Greiner are partially funded by the RE-INVEST project,

which is supported by the Innovation Fund Denmark under grant number 6154-00022B.

## Appendix A. Supplementary data

Supplementary data to this article can be found online at <https://doi.org/10.1016/j.esr.2021.100729>.

## Credit author statement

**Pablo Tapetado:** Data analysis, editing, original draft writing, software code preparation, investigation. **Marta Victoria:** Supervision, investigation, original draft writing, data analysis, methodology. **Martin Greiner:** Supervision, data-reviewing, methodology, manuscript-reviewing. **Julio Usaola:** Supervision, data-reviewing, manuscript-reviewing.

## References

- [1] Clean Energy for All Europeans | Energy, 2016. <https://ec.europa.eu/energy/en/topics/energy-strategy-and-energy-union/clean-energy-all-europeans>. (Accessed 19 July 2019). accessed.
- [2] Ministerio para la Transición ecológica y el Reto Demográfico, Plan Nacional Integrado de Energía y Clima 2021-2030, 2020. <https://www.miteco.gob.es/es/prensa/pniec.aspx>.
- [3] M. Victoria, C. Gallego-Castillo, Hourly-resolution analysis of electricity decarbonization in Spain (2017–2030), *Appl. Energy* 233–234 (2019) 674–690, <https://doi.org/10.1016/j.apenergy.2018.10.055>.
- [4] M.G. Rasmussen, G.B. Andresen, M. Greiner, Storage and balancing synergies in a fully or highly renewable pan-European power system, *Energy Pol.* 51 (2012) 642–651, <https://doi.org/10.1016/j.enpol.2012.09.009>.
- [5] G.B. Andresen, R.A. Rodriguez, S. Becker, M. Greiner, The potential for arbitrage of wind and solar surplus power in Denmark, *Energy* 76 (2014) 49–58, <https://doi.org/10.1016/j.energy.2014.03.033>.
- [6] E.H. Eriksen, L.J. Schwenk-Nebbe, B. Tranberg, T. Brown, M. Greiner, Optimal heterogeneity in a simplified highly renewable European electricity system, *Energy* 133 (2017) 913–928, <https://doi.org/10.1016/j.energy.2017.05.170>.
- [7] S. Kozarcanin, H. Liu, G.B. Andresen, 21st century climate change impacts on key properties of a large-scale renewable-based electricity system, *Joule* 3 (2019) 992–1005, <https://doi.org/10.1016/j.joule.2019.02.001>.
- [8] D. Connolly, H. Lund, B.V. Mathiesen, Smart Energy Europe: the technical and economic impact of one potential 100% renewable energy scenario for the European Union, *Renew. Sustain. Energy Rev.* 60 (2016) 1634–1653, <https://doi.org/10.1016/j.rser.2016.02.025>.
- [9] D.P. Schlachtberger, T. Brown, S. Schramm, M. Greiner, The benefits of cooperation in a highly renewable European electricity network, *Energy* 134 (2017) 469–481, <https://doi.org/10.1016/j.energy.2017.06.004>.
- [10] H.C. Gils, Y. Scholz, T. Pregger, D. Luca de Tena, D. Heide, Integrated modelling of variable renewable energy-based power supply in Europe, *Energy* 123 (2017) 173–188, <https://doi.org/10.1016/j.energy.2017.01.115>.
- [11] M. Huber, D. Dimkova, T. Hamacher, Integration of wind and solar power in Europe: assessment of flexibility requirements, *Energy* 69 (2014) 236–246, <https://doi.org/10.1016/j.energy.2014.02.109>.
- [12] F. Cebulla, T. Naegler, M. Pohl, Electrical energy storage in highly renewable European energy systems: capacity requirements, spatial distribution, and storage dispatch, *J. Energy Storage.* 14 (2017) 211–223, <https://doi.org/10.1016/j.est.2017.10.004>.
- [13] G. Pleßmann, P. Blechinger, How to meet EU GHG emission reduction targets? A model based decarbonization pathway for Europe's electricity supply system until 2050, *Energy Strateg. Rev.* 15 (2017) 19–32, <https://doi.org/10.1016/j.esr.2016.11.003>.
- [14] J. Ma, V. Silva, R. Belhomme, D.S. Kirschen, L.F. Ochoa, Evaluating and planning flexibility in sustainable power systems, *IEEE Trans. Sustain. Energy.* 4 (2013) 200–209, <https://doi.org/10.1109/TSTE.2012.2212471>.
- [15] M. Victoria, G.B. Andresen, Using validated reanalysis data to investigate the impact of the PV system configurations at high penetration levels in European countries, *Prog. Photovoltaics Res. Appl.* 27 (2019) 576–592, <https://doi.org/10.1002/ppp.3126>.
- [16] M. Victoria, Validated onshore and offshore wind time series for European countries (1979–2017), *Methods Descr.* (2019) 1–21, <https://doi.org/10.5281/zenodo.3245438>.
- [17] Red Eléctrica España (REE), ESIOS, 2017. <https://www.esios.ree.es/es>. (Accessed 26 August 2017). accessed.
- [18] Entso-E, ENTSO-E Transparency Platform, ENTSO-E, 2018. <https://www.entsoe.eu/data/data-portal/>. (Accessed 11 July 2019). accessed.
- [19] M. Victoria, K. Zhu, T. Brown, G.B. Andresen, M. Greiner, The role of storage technologies throughout the decarbonisation of the sector-coupled European energy system, *Energy Convers. Manag.* 201 (2019) 111977, <https://doi.org/10.1016/j.enconman.2019.111977>.